



**H2020 - Research and Innovation Action**

# APPLICATE<sup>\*</sup>

Advanced Prediction in Polar regions and beyond: Modelling, observing system design and Linkages associated with a Changing Arctic climaTE

Grant Agreement No: 727862

**Deliverable No. 1.3**

**Provision of novel metrics, which can be effectively determined from short time series, through ESMValTool**

## Submission of Deliverable

Work Package	WP1 Weather and climate model evaluation		
Deliverable No	D1.3		
Deliverable title	Provision of novel metrics, which can be effectively determined from short time series, through ESMValTool		
Version	1.0		
Status	Final		
Dissemination level	PU - Public		
Lead Beneficiary	8 - UCL		
Contributors	<input type="checkbox"/> 1 – AWI	<input type="checkbox"/> 2 – BSC	<input type="checkbox"/> 3 - ECMWF
	<input type="checkbox"/> 4 – UiB	<input type="checkbox"/> 5 – UNI Research	<input type="checkbox"/> 6 – MET Norway
	<input type="checkbox"/> 7 – Met Office	<input checked="" type="checkbox"/> 8 – UCL	<input type="checkbox"/> 9 - UREAD
	<input type="checkbox"/> 10 – SU	<input type="checkbox"/> 11 – CNRS-GAME	<input type="checkbox"/> 12 - CERFACS
	<input type="checkbox"/> 13 – AP	<input type="checkbox"/> 14 – UiT	<input type="checkbox"/> 15 - IORAS
	<input type="checkbox"/> 16 - MGO		
Due Date	31 October 2018		
Delivery Date	23 October 2018		



This project has received funding from the European Union's Horizon 2020 Research & Innovation programme under grant agreement No. 727862.

## Table of Contents

EXECUTIVE SUMMARY .....	4
1. INTRODUCTION .....	5
1.1. Background and objectives .....	5
1.2. Organisation of this report.....	5
2. METHODOLOGY.....	5
3. RESULTS AND DISCUSSION .....	7
4. CONCLUSIONS AND OUTLOOK .....	9
5. REFERENCES .....	9
6. ACRONYMS .....	10
7. ANNEXES.....	10

## EXECUTIVE SUMMARY

Field campaigns in the Arctic, like the ongoing Year Of Polar Prediction (YOPP, 2017-2019) or the upcoming Multidisciplinary drifting Observatory for the Study of Arctic Climate (MOSAIC, 2019-2020) are key opportunities to conduct an evaluation of Earth System Models (ESMs) at the process level. This raises, however, a number of challenges as ESMs are not necessarily in phase with the actual climate for periods as short as one or two years.

Here, a metric is developed to evaluate ESMs on their ability to simulate the snow and ice thicknesses and the underlying process of vertical heat conduction. The metric is derived from a diagnostic called the “heat conductivity index” that has the appealing property to be stable over time, and hence suitable for evaluation of Arctic sea ice where trends are generally strong and interannual variability high. The metric has been incorporated to the ESMValTool, a reference package for model evaluation. This will ensure wider use by the APPLICATE partners (WP1, 2, 4) but also by researchers analyzing the Coupled Model Intercomparison Project, phase 6 (CMIP6) dataset.

## 1. INTRODUCTION

### Background and objectives

The evaluation of sea ice in Earth System Models (ESMs) with in-situ data is in general not straightforward for several reasons. First, ESMs simulate the sea ice cover on grid cells that are several dozens of kilometres wide, while in-situ data are by definition highly localized. Second, ESMs are subject to internal climate variability, meaning that they are not supposed to replicate the exact observed values (sea ice thickness, concentration, snow depth...) at any given time and location. Another issue is that simulated sea ice biases are not necessarily reflecting errors in the sea ice models themselves, but can be the consequence of errors in the atmosphere and/or ocean components. These limitations call for new methods of evaluation that consider the ability of models to simulate processes rather than numbers, taking into account the large interannual variations that prevail at high latitudes.

The objective of Task 1.2.4 of APPLICATE is to propose novel diagnostics and metrics for the evaluation of sea ice in ESMs, recognizing the three aforementioned limitations and making use of as many in-situ field data as possible. Here, we show one example of such a metric. The metric has been developed consistently with the Model Assessment Plan (D1.1) criteria, reaching a balance between ease of physical interpretation, stability over time and availability of observational counterpart.

### Organisation of this report

We first introduce the physical rationale behind the diagnostic introduced here, named the Heat Conduction Index (Section 2). Then, we apply the HCI to both model data and in-situ observational data and propose a model evaluation based on this new index (Section 3). We propose perspectives in Section 4.

## 2. METHODOLOGY

In the Arctic and during the ice growing season (~October-April), new sea ice formation occurs chiefly by basal ice accretion, as a result of the imbalance between upward conductive heat fluxes and the ocean-ice heat flux. The ability of ESMs to correctly simulate heat conduction is therefore critical. However, measuring heat conduction is challenging. This process depends on a number of geophysical parameters, including the local snow and sea ice thicknesses, the air-ocean temperature contrast and the snow and ice conductivities. Evaluating these parameters individually in ESMs is challenging because of the lack of observational data, especially regarding the heat conductivities.

Instead of evaluating each parameter individually, we propose to study how they interact with each other. To this aim, we define the *Heat Conduction Index* as the dependence of interfacial snow-ice temperature  $T_i$  to the snow surface temperature  $T_s$ :

$$HCI = \frac{dT_i}{dT_s}$$

To first order, the HCI can be interpreted as the sensitivity of sea ice thermodynamics (summarized by the variable  $T_i$ ) to the atmospheric thermal forcing (summarized by the variable  $T_s$ ). High values of *HCI* indicate that the internal temperature of the snow-sea ice system follows closely the atmospheric forcing (the process of heat conduction is very efficient) while low values indicate a weak sensitivity (the process of heat conduction is not efficient).

It is straightforward to obtain  $T_i$  and  $T_s$  from ESM outputs, but less so from observations for a sufficiently long interval. Therefore, we reformulated HCI in terms of other state variables, namely snow and ice thickness. For this reformulation, a number of hypotheses were taken (Fig. 1): (1) the ice-snow system has no heat capacity (2) the temperature profile is linear through the snow and ice media (3) the basal ice temperature is constant, and (4) the snow and ice conductivities are constant. Under these assumptions, the HCI can be reformulated (full derivation in Annex) as:

$$HCI = \frac{k_s h_i}{k_s h_i + k_i h_s} \quad (\text{Eq. 1})$$

where  $k_s$  and  $k_i$  are the snow and ice heat conductivities, respectively, and  $h_s$  and  $h_i$  are the thickness of the snow and ice layers, respectively.

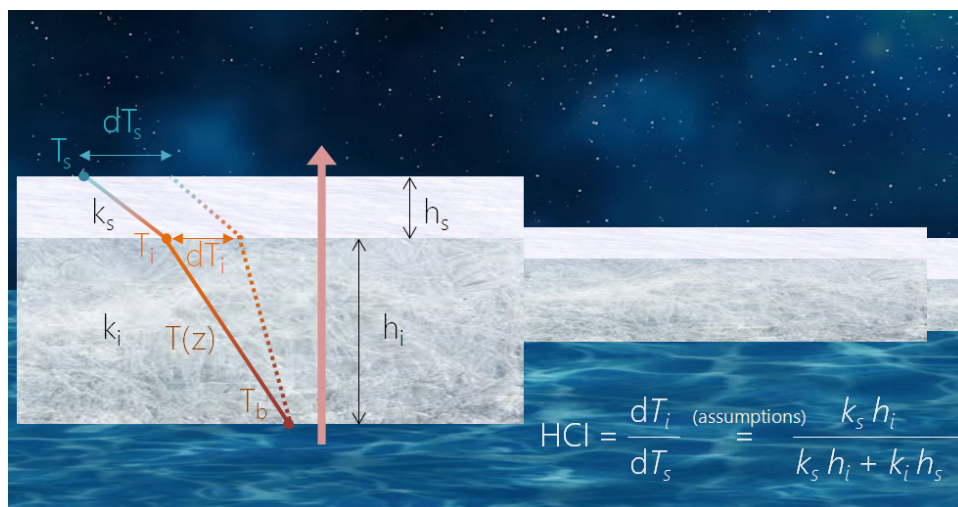


**Figure 1.** Simple view of vertical snow and sea ice thermodynamics in winter: a layer of snow sitting on a slab of ice, with no heat capacity, linear profiles of temperature and constant ice basal temperature.

Strictly speaking, the diagnostic given above does not measure the exact dependence of internal temperature to surface temperature, because of the assumptions above do not hold in reality. Yet, this diagnostic can be used in its own right to evaluate models, and in fact presents a number of advantages:

- Snow and ice thicknesses are standard geophysical parameters and they are well measured during field campaigns. The heat conductivities are less constrained and, if no estimate is available from the field, the same reference values can be used in models and observations;
- The HCI is designed to evaluate a process (heat conduction) rather than a single geophysical parameter (e.g., sea ice thickness or snow thickness individually). This means that an ESM with sea ice thickness twice as large as in observations could still simulate the right HCI value, provided the snow depth is also twice as large as in observations.
- The formulation of the HCI is simple and can be applied without running dedicated experiments: no new output variables are needed to evaluate the diagnostic. In particular, the HCI can be applied to existing models (CMIP3, CMIP5) as long as they have archived snow and ice thicknesses.

### 3. RESULTS AND DISCUSSION

#### 3.1 Stability of the Heat Conduction Index

In addition to the advantages listed above, a robust feature of the HCI is its high stability over time, despite strong secular trends in Arctic snow and ice thickness. It is clear from the definition of HCI (Eq. 1) that, if snow and ice thicknesses are each multiplied by the same constant factor, the HCI remains unchanged. In fact, the physics behind the process of heat conduction itself is not supposed to change in a warmer climate, when both the snow and ice covers are thinning. HCI is in fact more sensitive to the location where it is evaluated than on the year (Fig. 2). In Fram Strait where ice is relatively thin but snow relatively thick, HCI is in general lower than in other regions. HCI reaches even lower values in Antarctica, where the climatological ice and snow thicknesses are on average lower and higher than in the Arctic, respectively (due to larger ocean-ice heat flux and higher snow precipitation, respectively).

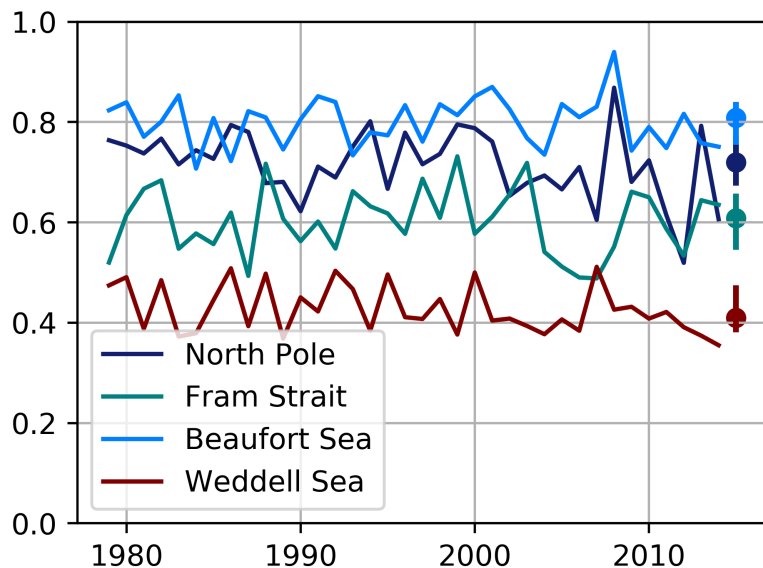


**Figure 2.** The Heat Conduction Index (Eq. 1) diagnosed from a 1979-2014 ocean-sea ice simulation (NEMO-LIM3 model) at four locations: North Pole, Fram Strait, Beaufort Sea and Weddell Sea. Error bars denote the median and the interquartile range of each time series.

The stability of HCI and its low signal-to-noise ratio make it a unique diagnostic for the study of the Arctic sea ice and also for the comparison between models and observations. Indeed, most – if not all – common sea-ice related diagnostics usually show strong trends and large interannual to decadal variability, which complicates model evaluation especially when it comes to coupled models. Here, even if the observational period is as short as one field campaign, the comparison can be meaningful because one year is, within a certain range, representative of the others – according to model results (Fig. 2). In the following, we apply the HCI to model output and observational data, and then compare them with each other.

#### 3.1 Diagnostic in models

All sea ice models output snow and ice thickness by default. The snow and ice conductivities that appear in the definition of HCI (Eq. 1) are taken by default to be 0.31 and 2.04 W/mK, following Maykut and Untersteiner (1971) and Lecomte et al. (2014). It is still possible to

prescribe other values for these parameters if those values are available from modelling groups. This should be the case for the upcoming CMIP6 data, as a full documentation on the models parameters was requested (Notz et al., 2015).

Here, for the purpose of illustration, we apply the HCI diagnostic to a 1979-2014 ocean-sea ice simulation conducted with the model NEMO-LIM3, following the protocol described in Barthélemy et al. (2016). In short, the ocean-sea ice model is run at a nominal resolution of  $1^\circ$  and forced by atmospheric reanalyses (DFS5.2; Dussin and Barnier, 2015). We evaluate HCI from the monthly mean values of actual snow and ice thicknesses (not the snow and ice volumes per unit grid cell area), since heat conduction depends on the actual thickness of the snow and ice layers, not on their grid cell average.

### 3.2 Diagnostic in observations

Contrary to model output, observations of snow and ice thickness are not available over decades nor on a regular grid. To emulate the context of ongoing or upcoming field campaigns like the YOPP or the MOSAiC, we analyze the Operation Ice Bridge (OIB) data over six one-day campaigns (2<sup>nd</sup>, 5<sup>th</sup>, 12<sup>th</sup>, 19<sup>th</sup>, 20<sup>th</sup>, 21<sup>st</sup> of April, 2010) that took place North of Greenland and the Canadian Arctic Archipelago (Fig. 3, left panel). OIB data (Kurtz and Farrell, 2011) are acquired by airborne radar instruments on aircrafts flying at ~500 m altitude and have a very high (~40 m) spatial resolution.

For each single measurement with non-zero snow and ice thicknesses, we evaluate the HCI following the formula above (Eq. 1) and take the same values for snow and ice conductivities as for models.

### 3.3 From diagnostic to metric: model-observation comparison

We map in Fig. 3 (left panel) the OIB sea ice thickness for the six one-day campaigns of April 2010 and for NEMO-LIM3 model output. The month of April was chosen as it is the one with the most observational campaigns, but also the month for which sea ice thickness and snow depth peak to their respective maxima (Hezel et al., 2012). Comparison between observed and modeled sea ice thickness reveals that the modeled sea ice thickness deviates significantly from the OIB data.

The HCI was then computed at a particular location in the Beaufort Sea (red cross of Fig. 3) in both the OIB data and from model output (Fig. 3, right panel), to mimic the situation of localized measurements that may happen during the YOPP Special Observing Periods or the MOSAiC. For the model output, we considered the one grid cell that contains the selected location. For the observational data, we included all April 2010 data that fell within  $\pm 0.5^\circ$  of latitude and longitude relative to the selected location. As this was the case for other locations, the model displays stable values of HCI over time in that region (Fig. 3, right). The comparison between model results and observations further suggests that, despite differences in sea ice thickness, the simulated and observed HCI are not inconsistent with each other.



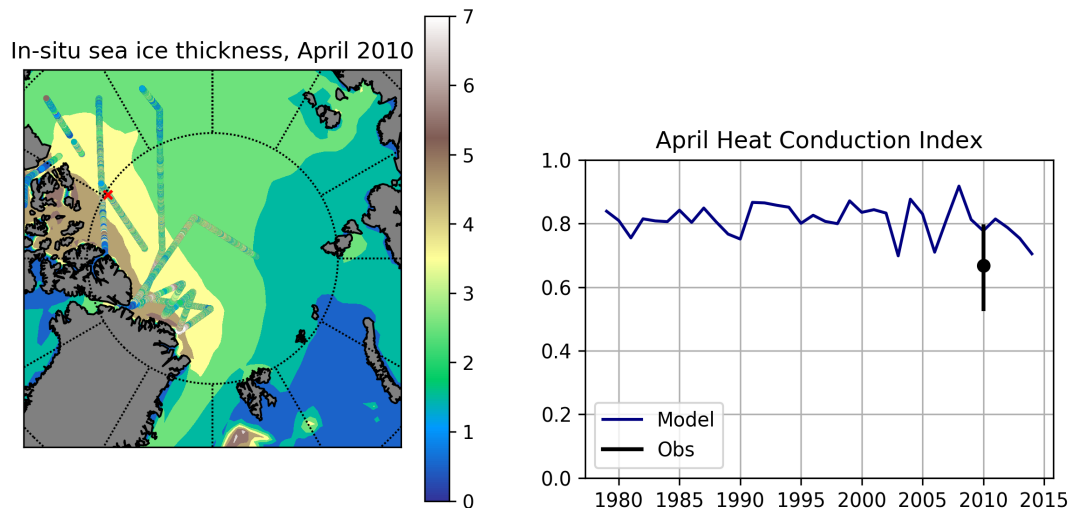


**Figure 3.** (Left) Sea ice thickness from Operation Ice Bridge (dots) for April 2, 5, 12, 19, 20 and 21, 2010, and from the ocean-sea ice model NEMO-LIM3 for April 2009 monthly mean (background). The red cross is the location where HCI is computed in the model – observations comparison in the right panel. (Right) Time series of simulated HCI in the grid cell that contains the red cross in the left panel, for April 1979-2014 (blue line) and the distribution of HCI from the 188,077 measurements that fell within 0.5° of the red cross during April 2010 in Operation Ice Bridge. The dot is the median and the bar is the interquartile range.

## 4. CONCLUSIONS AND OUTLOOK

The Heat Conduction Index is a first example of metric that can be used to bridge small-scale in-situ observations with large-scale output from climate models. The HCI is also an example of how climate models can be evaluated based on data from short field campaigns.

The HCI satisfies at least four of the six criteria that were listed in the Model Assessment Plan to make a “good metric”: interpretability (the metric evaluates a normalized snow/ice thickness that can be directly related to the sensitivity of internal thermodynamics to the atmospheric forcing); stability (the HCI is not much influenced by interannual variability); transparency (the HCI is coded in ESMValTool); and observability (the HCI can be estimated from field campaigns as long as snow and ice thickness estimates are available).

The next steps will be to apply this metric using data from the February-March 2018 YOPP Special Observing Periods and on a multi-model ensemble like CMIP6.

## 5. REFERENCES

Barthélemy, A., Goosse, H., Fichet, T., & Lecomte, O. (2017). On the sensitivity of Antarctic sea ice model biases to atmospheric forcing uncertainties. *Climate Dynamics*, 51(4), 1585–1603. <https://doi.org/10.1007/s00382-017-3972-7>

Dussin R, Barnier B, Brodeau L, Molines JM (2016) The making of the DRAKKAR Forcing Set DFS5. Drakkar/myocean report 01-04-16, Laboratoire de Glaciologie et de Géophysique

Hezel, P. J., Zhang, X., Bitz, C. M., Kelly, B. P., & Massonnet, F. (2012). Projected decline in spring snow depth on Arctic sea ice caused by progressively later autumn open

ocean freeze-up this century. *Geophysical Research Letters*, 39(17). <https://doi.org/10.1029/2012gl052794>

Kurtz, N. T., & Farrell, S. L. (2011). Large-scale surveys of snow depth on Arctic sea ice from Operation IceBridge. *Geophysical Research Letters*, 38(20). <https://doi.org/10.1029/2011gl049216>

Lecomte, O., Fichefet, T., Massonnet, F., & Vancoppenolle, M. (2015). Benefits from representing snow properties and related processes in coupled ocean–sea ice models. *Ocean Modelling*, 87, 81–85. <https://doi.org/10.1016/j.ocemod.2014.11.005>

Maykut, G. A., & Untersteiner, N. (1971). Some results from a time-dependent thermodynamic model of sea ice. *Journal of Geophysical Research*, 76(6), 1550–1575. <https://doi.org/10.1029/jc076i006p01550>

Notz, D., Jahn, A., Holland, M., Hunke, E., Massonnet, F., Stroeve, J., ... Vancoppenolle, M. (2016). The CMIP6 Sea-Ice Model Intercomparison Project (SIMIP): understanding sea ice through climate-model simulations. *Geoscientific Model Development*, 9(9), 3427–3446. <https://doi.org/10.5194/gmd-9-3427-2016>

## 6. ACRONYMS

CMIP	Coupled Model Intercomparison Project
HCI	Heat Conduction Index
MOSAIC	Multidisciplinary drifting Observatory for the Study of Arctic Climate
OIB	Operation Ice Bridge
YOPP	Year Of Polar Prediction

## 7. ANNEXES

### Formula for the Heat Conduction Index

Assuming constant snow and ice conductivities, fixed basal ice temperature and linear vertical profiles of temperature through the sea ice and snow media, the heat conduction fluxes through snow and sea ice are given by Fourier's heat conduction law:

$$q_i = -k_i \frac{T_i - T_b}{h_i} \text{ and } q_s = -k_s \frac{T_s - T_i}{h_s}$$

where  $q_i$  and  $q_s$  denote the heat conduction through the ice and snow media, respectively;  $T_s$ ,  $T_i$  and  $T_b$  denote the snow-atmosphere, ice-snow and ocean-ice interfacial temperatures, respectively (Fig. 1 of the main text);  $k_s$  and  $k_i$  denote the snow and ice conductivities, respectively; and  $h_s$  and  $h_i$  the snow and ice thicknesses, respectively. Assuming no phase change at the ice-snow interface, the conservation of energy implies  $q_i = q_s$ . Solving for  $T_i$ , one has

$$\begin{aligned} k_i h_s (T_i - T_b) &= k_s h_i (T_s - T_i) \\ (k_i h_s + k_s h_i) T_i &= k_s h_i T_s + k_i h_s T_b \end{aligned}$$

In that particular case, the heat conduction index, as initially defined in the text, becomes:

$$HCI = \frac{dT_i}{dT_s} = \frac{k_s h_i}{k_i h_s + k_s h_i}$$

### Python function evaluating the Heat Conduction Index

This function is also available from the ESMValTool.

```
#!/usr/bin/python

# Author:      Francois Massonnet

# Date:        August 2018

# Purpose:     Function to make first-order evaluation
#              of heat conduction

# Reference:   APPLICATE Deliverable 1.3

#

# Module imports

from netCDF4 import Dataset

import numpy as np

import scipy.stats

import esmvaltool.interface_scripts.preprocess

import iris

import logging

import sys

logger = logging.getLogger(__name__)

def hci(sithick, snthick, ki = 2.034, ks = 0.31 ):

    """ Function hci(sithick, snthick, ki = 2.034, ks = 0.31 )

        Inputs:      sithick: 2-D numpy array of

                                actual sea ice thickness (as one
                                would measure it) in [m]

                    snthick: 2-D numpy array of

                                actual snow thickness (as one
                                would measure it) in [m]

                    ki      : 2-D numpy array of

                                sea ice conductivity [W/m/K]

                                If not provide, takes default
```

```

        value of 2.034 W/m/K (Maykut and Untersteiner, 1971)

ks      : 2-D numpy array of

        snow ice conductivity [W/m/K]

        If not provide, takes default

        value of 0.31 W/m/K (Lecomte et al., 2015)

Output:   hci: Heat Conduction Index =

        ks * sithick / (ks * sithick + ki * snthick)

        For the Semtner 0-layer model, HCI is exactly

        equal to the derivative of interfacial snow-ice

        temperature to the surface temperature.

        HCI is a first-order measure of the way that the

        system's dynamics responds to the forcing.

        HCI is reported as NaN where both thicknesses

        are zero

"""

if (type(sithick) != np.ndarray and type(sithick) != np.float64) or \
    (type(snthick) != np.ndarray and type(snthick) != np.float64):
    raise TypeError("(hci) Input arguments are not numpy arrays")

if sithick.shape != snthick.shape:
    raise ValueError("(hci) Input arrays dimensions don't match")

# Create masked array to not have data for regions where there is no ice
mask_noice = 1.0 * (sithick * snthick == 0)

sithick = np.ma.masked_array(sithick, mask = mask_noice)

snthick = np.ma.masked_array(snthick, mask = mask_noice)

output = ks * sithick / (ki * snthick + ks * sithick)

return output

```